DOI: 10.1021/ma101620k

Macromolecules
ARTICLE

Confinement Effects on Watery Domains in Hydrated Block Copolymer Electrolyte Membranes

Sung Yeon Kim[‡] and Moon Jeong Park*[,†,‡]

[†]*Department of Chemistry and* [‡]*Division of Advanced Materials Science, Pohang University of Science and Technology (POSTECH), Pohang, Korea 790-784*

Nitash P. Balsara

Department of Chemical Engineering, Materials Sciences Division, and Environmental Energy Technologies Division, Lawrence Berkeley National Laboratory, University of California, Berkeley, California 94720

Andrew Jackson

NIST Center for Neutron Research, National Institute of Standards and Technology, Gaithersburg, Maryland 20899, and Department of Materials Science and Engineering, University of Maryland, College Park, Maryland 20742

Received July 19, 2010; Revised Manuscript Received August 13, 2010

ABSTRACT: The morphology of a series of diblock copolymers comprising randomly sulfonated polystyrene (PSS) and polymethylbutylene (PMB) blocks equilibrated with humid air was determined by *in situ* small-angle neutron scattering (SANS). *In-situ* SANS data were collected over a wide angular range permitting the determination of the superstructure of the hydrophilic PSS-rich and hydrophobic PMB-rich domains and the substructure within the hydrophilic PSS-rich domains. When the characteristic length of the superstructure is larger than 10 nm, the hydrophilic PSS domains are heterogeneous with periodically arranged watery domains. The scattering signature of the watery domains is very similar to the well-established "ionomer peak". This peak vanishes when the neutron scattering length density of the water (H_2O/D_2O mixture) is matched to that of the PSS block. The spacing between watery domains depends only on sulfonation level of the PSS block. When the characteristic length of the superstructure is less than 10 nm, the watery substructure disappears and homogeneous hydrated PSS-rich domains are obtained.

Introduction

Proton exchange fuel cells (PEFCs) have the potential to provide power for a variety of applications such as portable electronics and transportation vehicles. One of key components in PEFC is the polymer electrolyte membrane (PEM), which serves as medium for transporting protons from the anode to the cathode.[1−3] The most widely investigated PEMs are obtained from random copolymers of perfluorosulfonic acid (PFSA) ionomer (commercialized under the trademark Nafion).[1−4] Another class of PEMs gaining increasing attention are sulfonated polymers containing aromatic phenyl ring such as sulfonated poly(ether ether ketone) (SPEEK) and poly(aryl ether ketone) (SPAEK)[5,6] due to their high conductivity and electrochemical stability. These materials belong to a wide class of polymers that are often referred to as "ionomers" wherein ionic moieties are randomly located along the backbone of a hydrophobic polymer. In most cases, the ion-containing monomers aggregate, giving rise to a scattering peak with a characteristic length scale in the 3−5 nm.[7,8] It is generally agreed that in dry ionomers this "ionomer peak", as it is ubiquitously referred to, is a measure of the distance between adjacent ionic aggregates. In conventional ionomers the ionic aggregates serve as physical cross-links and improve the mechanical properties of the polymer. In PEMs, the ionic aggregates trap water from the surrounding air, which enables proton transport when the channels form a percolating network. The relationship between the characteristics of the ionomer peak, which persists upon hydration, and the proton transport in PEMs is a subject of long-standing debate.[9−14]

One of the problems with PEMs based on random copolymers is the fact that the morphologies obtained in both the dry and hydrated states are highly disordered. In most cases, physical models are built on the basis of the scattering profiles comprising the ionomer peak at high scattering angles and low angle tails that are consistent with power laws over a limited range on angles. There is, for example, little agreement on the basic morphology of the hydrated channels in Nafion.[11−18] The early hypothesis of the "dumbbell model" suggested by Gierke,[11,15] where spherical nodules 4−5 nm in diameter are interconnected by 1 nm wide channels, has given way to simpler morphologies including a layered morphology,[16,17] interconnected network of channels,[2,13,18] and noninterconnected cylindrical water channels.[14] In most models, it is argued that the ionomer peak obtained in hydrated samples gives the distance *between* the hydrated channels.[14−18] An interesting model proposed by Nieh et al. suggests that the ionomer peak in hydrated samples gives the distance between water-rich domains *along* the hydrated channels.[19] Additional difficulties arise due to the crystalline nature of most random copolymer-based PEMs. In these cases, the hydrated channels coexist with lamellar crystals that are arranged in superstructures such as "fringed micelles" and

*Corresponding author. E-mail: moonpark@postech.edu.

 Published on Web 09/01/2010 © 2010 American Chemical Society

"spherulites". Since these superstructures are always out of equilibrium, it is not known if the observed morphological trends are due to equilibrium self-assembly or a highly constrained out-of-equilibrium response of the morphology to changes in thermodynamic driving forces.

Block copolymers with hydrophilic and hydrophobic blocks such as sulfonated poly(styrene-*b*-isobutylene-*b*-styrene) (S-SIBS),[20] sulfonated poly(styrene-*b*-[ethylene-*co*-butylene]-*b*-styrene) (S-SEBS),[21] and sulfonated poly([vinylidene difluoride-*co*-hexafluoropropylene]-*b*-styrene) (P(VDF-*co*-HFP)-*b*-SPS)[22] can also be used to create PEMs. These materials belong to a broad class of compounds that can self-assemble into ordered domains with well-defined morphologies. When these materials are hydrated, the water molecules and hydronium ions are expected to be preferentially located within the hydrophilic PSS domain. A common feature that these systems share with the random copolymer-based PEMs is the fact that the hydrophilic block is a random copolymer of sulfonated and non-sulfonated monomers. One thus expects ionomer peaks to arise in these systems that are qualitatively similar to those obtained in random-copolymer-based ionomers. Several studies have reported the presence of hierarchical structures, ordered domains with characteristic lengths in the 30−40 nm range, and hydrated ionomer peaks with characteristic lengths in the 2−6 nm range.[19,23−25] The scattering peaks indicative of both structures reduce in intensity as the sulfonation level or hydration level is increased, indicating a disordering of the morphology on both length scales. Since the extreme thermodynamic incompatibility of sulfonated monomers in non-sulfonated monomers is well-established,[26,27] thermodynamic self-assembly would have led to the opposite result.

In the case of materials like Nafion and SPEEK, the sulfonated groups can lie anywhere along the chain, while in the S-SIBS like materials, the sulfonated groups are confined to specific locations such as the end blocks of the S-SIBS chains. To distinguish clearly between the two systems, we refer to the Nafion-like materials as randomly sulfonated homopolymers and the S-SIBS-like materials as randomly sulfonated block copolymers. To our knowledge, there is no evidence for the formation of channels or domains comprising only sulfonic acid groups and water in these systems. It is generally understood, for example, that a significant number of nonionic monomers are trapped within the ionic aggregates in ionomers. Because of the proximity of hydrophobic and hydrophilic groups along the polymer chain and due to the significant entropic barriers for perfect segregation the hydrophobic and hydrophilic groups in both cases,[28] it is likely that the proton-conducting channels contain a significant concentration of hydrophobic groups. When we refer to "hydrophilic domains", it should be understood that the domains are rich in sulfonated groups and water but that they probably contain a significant concentration of hydrophobic monomers. There is, of course, the possibility that these nominally hydrophilic PSS domains are not homogeneous but rather contain a water-rich and water-poor substructure. We thus anticipate the presence of two length scales: one characterizing the nominally hydrophilic PSS domain superstructure, d, and one characterizing the heterogeneous water substructure, d_{water}.

This paper is part of a series on randomly sulfonated block copolymer PEMs system comprising nominally hydrophilic sulfonated polystyrene (PSS) blocks and hydrophobic polymethylbutylene (PMB) blocks.[27,29,30] In previous studies, the size and shape of the hydrophilic PSS domains were varied by varying the chain length and PSS volume fraction in the PSS-*b*-PMB copolymers. In particular, we found that small hydrophilic PSS domains with widths less 6 nm were more effective in retaining water at elevated temperatures. This had a marked effect on proton transport which increased with decreasing channel size. Our work thus far has focused on the overall dimensions of the nominally hydrophilic and hydrophobic domains which was studied by small-angle neutron and X-ray scattering (SANS and SAXS) and electron microscopy. As with other studies involving block copolymers, the PSS blocks in our system were obtained by random sulfonation. The purpose of the present paper is to present neutron scattering data from PSS-*b*-PMB copolymers equilibrated with humid air at both low and high scattering angles to simultaneously capture changes in both d and d_{water}. The formation of well-defined morphologies greatly simplifies our interpretation of the scattering data. The implication of our results on previously drawn conclusions on proton-conducting PEMs is discussed.

Experimental Section[36]

Polymer Synthesis and Characterization. A series of poly(styrenesulfonate-*b*-methylbutylene) (PSS-*b*-PMB) copolymers were synthesized and characterized following procedures given in ref 27. The number-averaged total molecular weights of PSS-*b*-PMB copolymer are ranging from 9.4 to 115.5 kg/mol. We use the term P4, P9, P17, and P48 to refer to these polymers where the integers indicate the nominal molecular weight of precursor PS block (before sulfonation) in kg/mol. Samples with different sulfonation levels (SLs) were prepared by controlling sulfonation reaction time. Samples are then labeled according to the SL; for example, P48(31) has PSS domains where 31 mol % of PS chains are sulfonated.

***In-Situ* Small-Angle Neutron Scattering (*In-Situ* SANS).** The SANS samples were prepared by solvent casting the polymer from THF solutions on 1 mm thick quartz windows. The sample thickness ranged from 110 to 170 μm, and a circular area with a diameter of 1.8 cm was exposed to the neutron beam. The samples were studied using the 30 m NG3 beamline at the National Institute of Standards and Technology (NIST) equipped with a sample holder wherein the humidity of the surrounding air and sample temperature were controlled. Water from a well located within the sample chamber is used to humidify the air around the sample. In our experiments, the well was filled with pure D_2O or D_2O/H_2O mixtures. The wavelength of the incident neutron beam (λ) was 0.6 nm ($\Delta\lambda/\lambda = 0.10$), and two different sample-to-detector distances of 1.0 and 12.0 m were used. This enabled access to scattering at q values in the range 0.03−6.0 nm^{-1}. The highest temperature and RH limit of the NIST humidity sample chamber are $T = 75$ °C and RH = 98%, respectively. Separate transient measurements were conducted as a function of sample thickness to ensure adequate equilibration time for the temperature and humidity steps used in our study.

Water Uptake Measurements. Polymer films with thickness ranging from 50 to 70 μm were prepared by solvent casting from 10 wt % THF solutions. The films were dried at room temperature for 3 days under a N_2 blanket and under vacuum at 60 °C for 5 days. Prior to water uptake experiment, the films were exposed to vacuum for 24 h and then hooked on the end of the quartz spring balance (RUSKA, spring constant $k = 4.9$ mN/m), located in an ESPEC SH-241 humidity chamber equipped with specially designed glassware to prevent breakage of the quartz spring due to air flow in the humidity chamber. The spring is nonrotating and has a reference pointer, which is used to measure the increment of total length of the spring upon hydration. At fixed humidity of 98%, samples were studied as a function of temperature ranging from 25 to 60 °C. The degree of hydration, λ, is computed as follows:

$$\lambda = \frac{[H_2O]}{[SO_3H]} = \frac{\text{mol of water absorbed/1 g of dry PSS}-\text{PMB}}{\text{mol of sulfonated styrene/1 g of dry PSS}-\text{PMB}} \quad (1)$$

Transmission Electron Microscopy (TEM). The PSS−PMB samples prepared by the same method used to prepare the water

Table 1. Materials Used in the Present Study

sample code[a]	mol wt (PSS−PMB) (g/mol)	ϕ_{PSS}	SL (%)	morphology in dry state	domain spacing in dry state[b] (nm)
P48(19)	55.7K−55.0K	0.440	19	LAM	74.9
P48(31)	60.5K−55.0K	0.448	31	HEX	78.3
P17(20)	19.3K−18.7K	0.443	20	HEX	41.4
P17(29)	20.5K−18.7K	0.449	29	HEX	41.7
P17(42)	22.3K−18.7K	0.458	42	HEX	42.5
P9(19)	10.6K−8.7K	0.484	19	LAM	20.6
P9(53)	13.2K−8.7K	0.509	53	HEX	22.1
P4(44)	5.3K−4.1K	0.475	44	HEX	11.4

[a] Samples are labeled according to the nominal molecular weight of the non-sulfonated PS block and the SL value. Sample P48(19), for example, is the PSS−PMB block copolymer with a 48 kg/mol PS block with SL = 19 mol %. [b] The values are determined from SAXS experiments performed under vacuum.

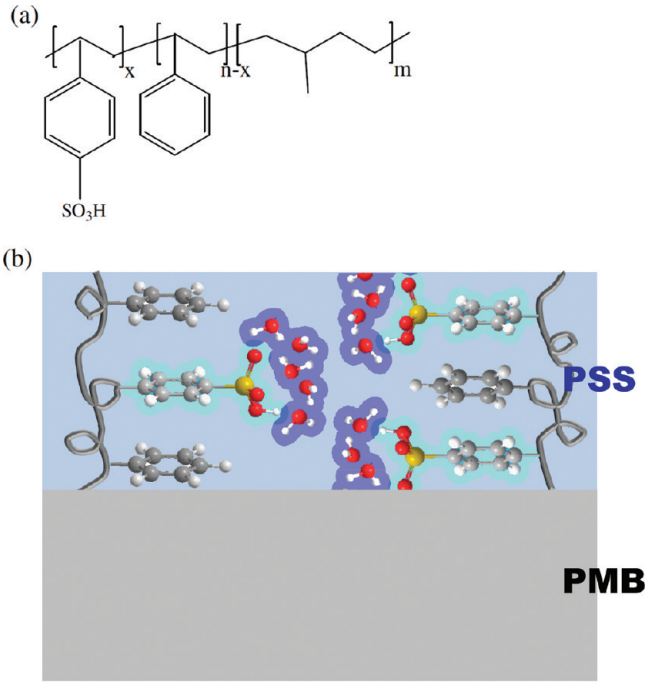

Figure 1. (a) Molecular structure of PSS-*b*-PMB copolymer and (b) schematic illustration of a hydrated PSS-*b*-PMB membrane.

uptake samples were cryo-microtomed at −100 °C to obtain thin sections with thicknesses in the 50−80 nm range using an RMC Boeckeler PT XL ultramicrotome. The electron contrast in the dry polymer samples was enhanced by exposure to ruthenium tetroxide (RuO_4) vapor for 50 min. Imaging of stained samples was performed with a Zeiss LIBRA 200FE microscope operating at 200 kV equipped with a cold stage (−160 °C) and an Omega energy filter. Images were recorded on a Gatan 2048 × 2048 pixel CCD camera (Gatan Inc., Pleasanton, CA).

Results

The characteristics of PSS-*b*-PMB copolymers used in this study are listed in Table 1. All copolymers are in acidic form (H^+), and Figure 1a shows the molecular structure of the polymers. The morphologies of the dry polymers and the domain spacings, d, are summarized in Table 1. The d is defined as $2\pi/q^*$, where q^* is the magnitude of the scattering vector at the primary peak. Most of the samples show hexagonally packed cylinder morphology (HEX) in dry state, except for the lightly sulfonated copolymers which show a lamellar structure. Figure 1b shows schematic illustration of a hydrated PSS−PMB membrane. In the presence of humid water vapor, the hydrophilic PSS domains selectively absorb water molecules from air to yield the substructure of hydrophilic PSS domains, i.e., segregation of the hydrated ionic groups within.

Typical TEM results are shown in parts a, b, and c of Figure 2, where micrographs of dry P4(44), P9(53), and P17(42), respectively, are shown. In all cases PMB cylinders surrounded by PSS matrices are observed. The domain spacings measured by SAXS (data not shown here for brevity) and TEM are in reasonable agreement. From the TEM images in Figure 2, the widths of PSS domains (darkened by exposure to RuO_4) are estimated to be 6 nm (P4(44)), 11 nm (P9(53)), and 21 nm (P17(42)). These values are not markedly different from one-half of domain sizes listed in Table 1.

Results of water uptake measurements on P48(31) as a function of temperature at RH = 98% are shown in the inset of Figure 3. It is evident that the degree of hydration, λ, increases monotonically with increasing temperature, as seen in previous studies on similar systems.[29] Figure 3 shows *in-situ* SANS data from P48(31) sample exposed to D_2O/air environment at different RHs and temperatures. After changing the temperature and RH of surrounding air, the sample was annealed for 2 h at each condition, which is needed to establish equilibrium. The equilibration time was determined by noting the time required for the primary peak intensity to reach a time-independent plateau. We used two different sample-to-detector distances of 12 and 1 m to cover a wide range of scattering vectors. The SANS profiles obtained from the two configurations, with darker (12 m)−brighter (1 m) colored profiles, are spliced together with no adjustable parameters. Scattering peaks at $1q^*$, $\sqrt{3}q^*$, $\sqrt{4}q^*$, $\sqrt{7}q^*$, $\sqrt{9}q^*$, $\sqrt{11}q^*$, and $\sqrt{12}q^*$, as shown by the inverted open triangles ($\triangledown$), over the entire range of conditions studied indicate the presence of a HEX phase. At low temperature (25 °C) and low humidity (RH = 25%) conditions, the domain spacing of the nominally hydrophilic PSS domains corresponding to the spacing between the {100} planes, d = 78.3 nm. D_2O molecules associate primarily with the PSS-rich domains, and therefore, increased water uptake results in an increase in the neutron scattering contrast between the PSS-rich and PMB-rich regions. At RH = 95% and 40 °C, a broad shoulder in the vicinity of q = 1.8 nm^{-1} is seen. The intensity of the shoulder significantly increases upon further heating and humidification. At T = 60 °C, a clear peak at q = 1.74 nm^{-1} is evident. The location of this peak is similar to the "ionomer peak" seen in previous studies.[12−20] However, in our case, this peak arises only upon hydration, and we thus tentatively refer to it as the "water peak". We refer to $2\pi/q_{water}$ as the water domain spacing, d_{water}, where q_{water} is the location of the water peak along the q axis. Heating the P48(31) sample from 40 to 60 °C in humid air leads to an increase in the d_{water} from 3.4 to 3.6 nm (6% increase) and concomitant swelling of PSS−PMB microphase from d = 81.5 to 84.5 nm (4% increase).

Figure 4 shows *in-situ* SANS profiles of P17 samples with SL = 20%, 29%, and 42%. The SANS profiles obtained at dry state at RH = 25% and 60 °C are compared to those obtained in the hydrated at RH = 95% and 60 °C using D_2O for humidification. In all cases we see the absence of the water peak in the dry state

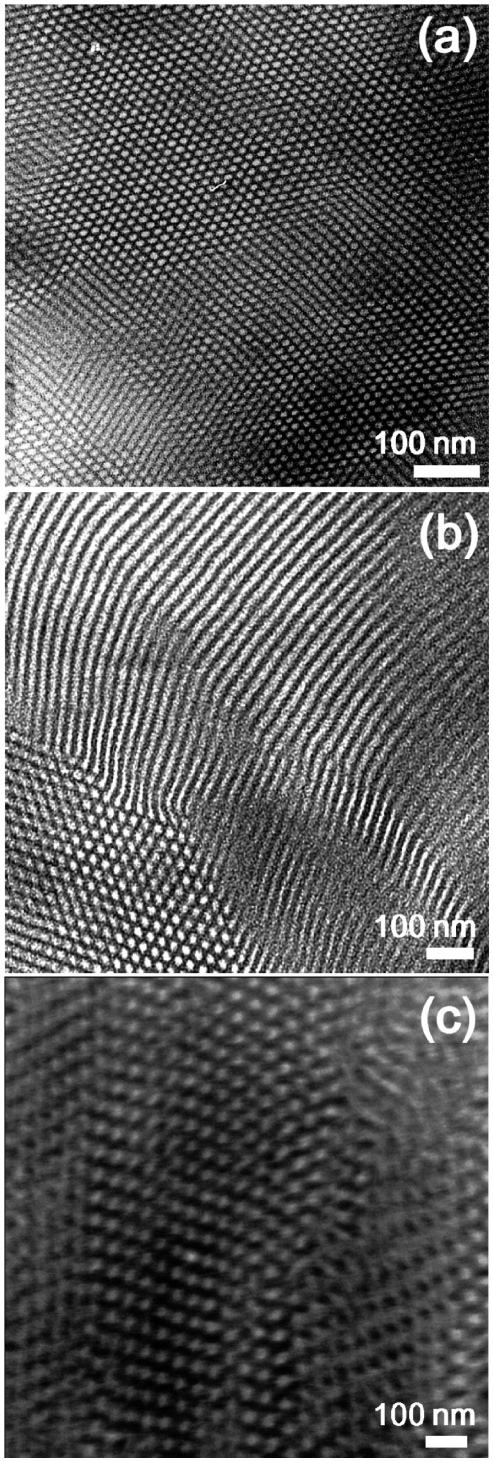

Figure 2. Cross-sectional TEM image of (a) P4(44), (b) P9(53), and (c) P17(42) showing PMB cylinders surrounded by PSS matrices. PSS domain was darkened by RuO_4 staining.

and the emergence of the water peak upon hydration. In addition, there is a strong correlation between SL and the location of the water peak. Increasing SL from 20 to 42 mol % results in a decrease in water domain spacing from 4.2 to 3.0 nm. This is certainly reasonable as the average distance between SO_3^- groups decreases with increasing SL. Our work is distinguished from the results of Frisken et al.[23] where the opposite trend is reported; i.e., the water domain spacing of fully hydrated membranes increases with increasing sulfonation level. Another distinction of the present work is the presence of multiple peaks in the SANS

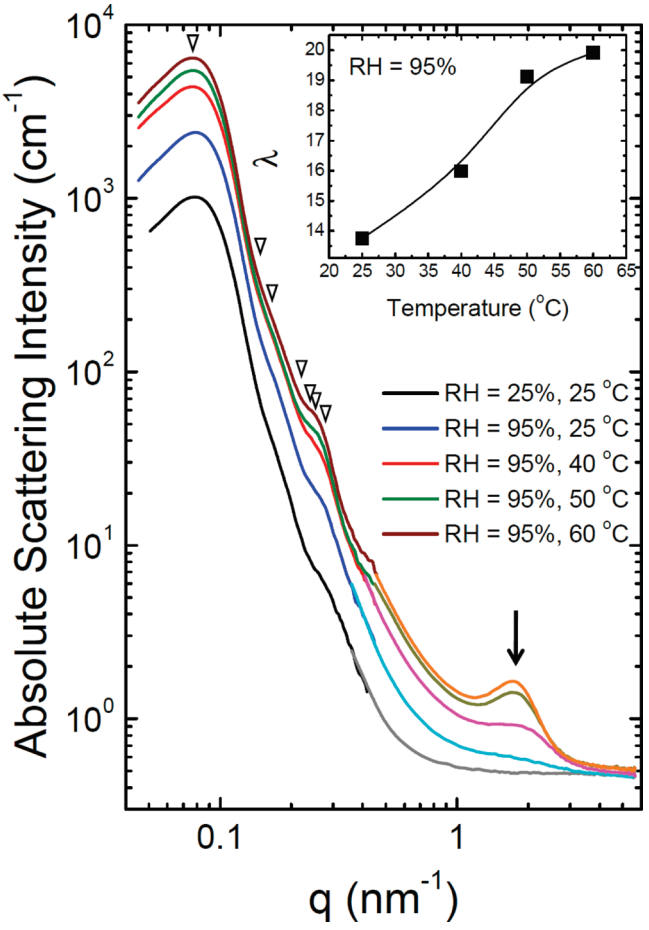

Figure 3. *In-situ* SANS profiles of P48(31) exposed to D_2O/air environment at different RH and temperature showing Bragg peaks at $1q^*$, $\sqrt{3}q^*$, $\sqrt{4}q^*$, $\sqrt{7}q^*$, $\sqrt{9}q^*$, $\sqrt{11}q^*$, and $\sqrt{12}q^*$; the inverted open triangles (▽) reveal hexagonal cylinder morphology. When the temperature is increased at fixed RH = 95%, the formation of water domain is seen as indicated by the arrows (↓). The scattering profiles are obtained with two different sample-to-detector distances of 12 and 1 m as overlaid with darker and brighter colored curves, respectively. Inset plots show degree of hydration, λ, as a function of temperature at RH = 95%.

profiles that enables quantitative determination of the arrangement of the nominally hydrophilic PSS domains that form the matrix of a HEX phase. In contrast, the randomly sulfonated homopolymers only show scattering tails in this window.

One can claim that the absence of high-q peak in dry state is simply due to the low scattering contrast to see the peak with low concentration of D_2O whether the structure is present or not. However, the fact that we were not able to see the high-q peak for all of the samples at RH = 75% regardless of water uptakes of the samples leads us to conclude that the lack of water is not the reason for the absence of high-q peak. For example, the degree of hydration of P9(53) at RH = 75% and T = 60 °C is λ = 11; however, no detectable peak at high q is observed. In contrast, although the degree of hydration of P17(20) at RH = 95% and T = 60 °C is as small as λ = 9, there exists clear peak at high q as shown in Figure 4.

We now describe the results of a key experiment to determine the origin of the water peak. The SLDs of PS and sulfonated PS (SL = 100%) are 1.41×10^{-4} and 2.05×10^{-4} nm^{-2}, respectively, while that of D_2O and H_2O is 6.37×10^{-4} and -0.56×10^{-4} nm^{-2}, respectively. The D_2O/H_2O ratio in the surrounding air can be used to control SLD of water within the PSS, assuming that water uptake is unaffected by deuterium substitution. The SLD of a 32/68 volumetric D_2O/H_2O mixture (1.65×10^{-4} nm^{-2})

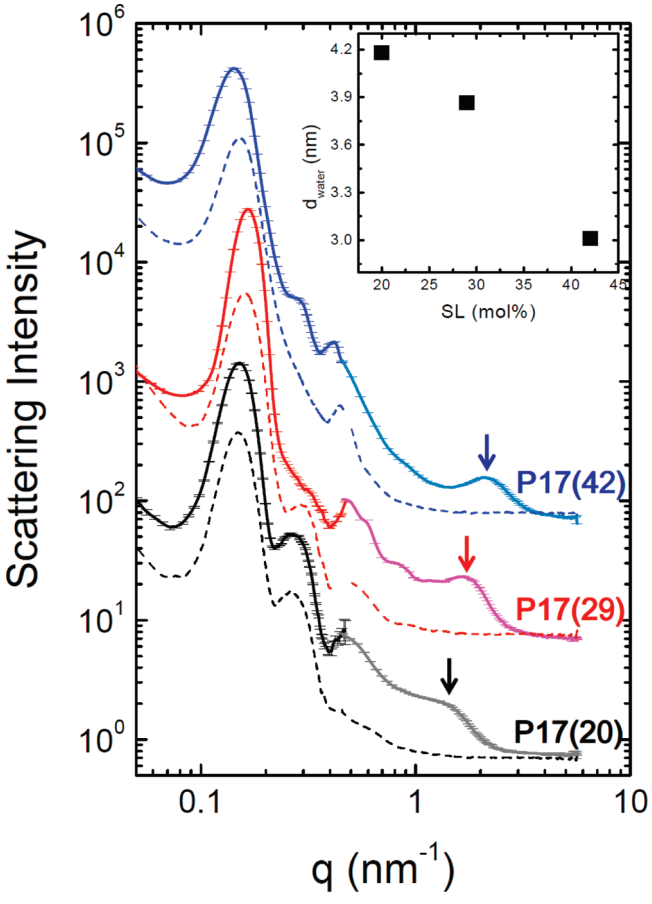

Figure 4. *In-situ* SANS intensity versus magnitude of the scattering vector, q, of hydrated P17(20), P17(29), and P17(42) obtained at RH = 95% and 60 °C (solid curves). The scattering profiles obtained with two different sample-to-detector distances of 12 and 1 m are shown as darker and brighter colored curves, respectively. The dashed curves below each hydrated SANS profile correspond to the SANS profile obtained in the dry state at RH = 25% and 60 °C. Scattering profiles of P17(29) and P17(42) are offset vertically by factors of 10 and 10^2 for clarity. The inset shows d_{water} vs SL.

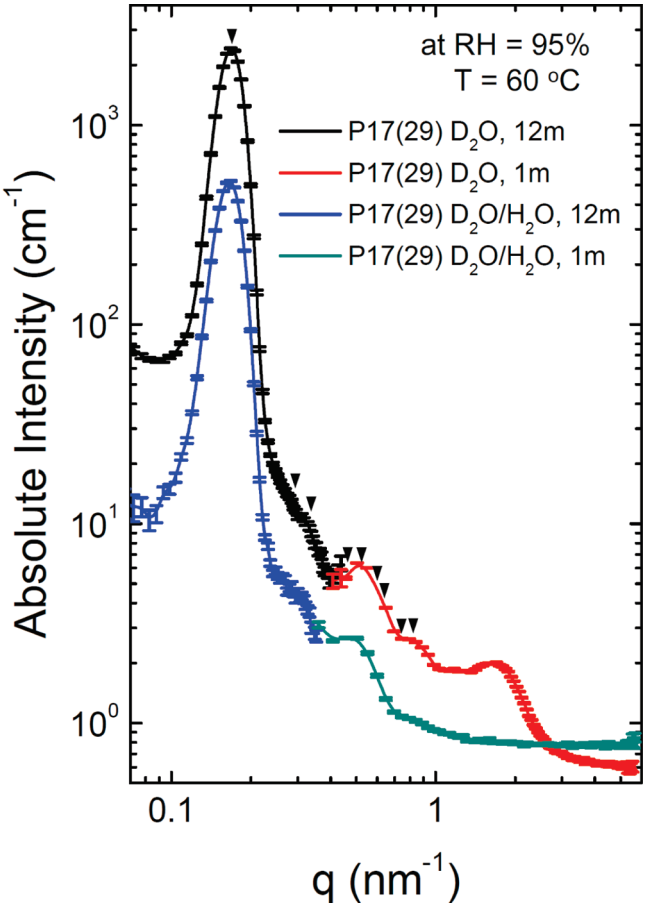

Figure 5. *In-situ* SANS intensity versus magnitude of the scattering vector, q, of P17(29) obtained at RH = 95% and 60 °C with (a) 100% D_2O and (b) 32/68 volumetric D_2O/H_2O mixture. The scattering profiles showing Bragg peaks at q/q^* ratios of 1, $\sqrt{3}$, $\sqrt{4}$, $\sqrt{7}$, $\sqrt{9}$, $\sqrt{11}$, $\sqrt{12}$, $\sqrt{16}$, and $\sqrt{24}$ are obtained with two different sample-to-detector distances of 12 and 1 m.

is nearly identical to the SLD of a dry PSS block with SL = 29% (1.63×10^{-4} nm^{-2}).

Figure 5 shows *in-situ* SANS profiles for P17(29) samples equilibrated with air containing pure D_2O and a 32/68 volumetric D_2O/H_2O mixture at the RH = 95% and 60 °C. The water peak seen clearly in the pure D_2O sample vanishes when the D_2O/H_2O mixture is used to humidify the air. In both cases, the SANS profiles reveal most of the expected Bragg peaks (▼) at $1q^*$, $\sqrt{3}q^*$, $\sqrt{4}q^*$, $\sqrt{7}q^*$, $\sqrt{9}q^*$, $\sqrt{11}q^*$, $\sqrt{12}q^*$, $\sqrt{16}q^*$, and $\sqrt{24}q^*$ with $q^* = 0.16$ nm^{-1} indicative of a HEX morphology. The low contrast between the PMB-rich hydrophobic and PSS-rich hydrophilic domains obtained in the D_2O/H_2O mixtures precluded detection of the $\sqrt{24}q^*$ Bragg peak. It is obvious that the water peak arises from a substructure within the PSS superstructure. This is consistent with the hypothesis of Nieh et al.[19]

The same experimental protocol is repeated with P48(31) samples as shown in Figure 6. In good agreement with P17(29) sample, the water peak clearly disappears when the D_2O/H_2O mixture is used to humidify the air while keeping the same Bragg peaks (▼) at $1q^*$, $\sqrt{3}q^*$, $\sqrt{4}q^*$, $\sqrt{7}q^*$, $\sqrt{9}q^*$, $\sqrt{11}q^*$, and $\sqrt{12}q^*$. While the data in Figures 5 and 6 prove the presence of water-rich and water-poor domains with an average spacing of 39 and 78 nm, it does not imply the presence of isolated pools of pure water surrounded by dry PSS chains. The neutron scattering contrast between the watery and PSS-rich domains is eliminated regardless of the concentrations of the two domains. Determining the concentration of the water-rich and water-poor domains will require a more extensive study. In addition, we have no evidence for the presence of ionic clusters in the dry PSS-*b*-PMB copolymers. Such data may be obtained by replacing protons with heavier cations,[31] which is a subject of future study.

Figure 7 compares *in-situ* SANS profiles of P4(44) obtained in the dry state at RH = 25% and 60 °C with those obtained in the hydrated state at RH = 95% and 60 °C using D_2O for humidification. Both profiles show Bragg peaks (▼) at $1q^*$, $\sqrt{3}q^*$, and $\sqrt{4}q^*$, indicative of the HEX phase but a remarkable absence of the water peak in the vicinity of $q = 1.8$ nm^{-1}. The degree of hydration at RH = 95% and 60 °C of P4(44) is 22.5, which is larger than that of all of the other samples examined. It is thus again clear that the lack of water is not the reason for the absence of the water peak in P4(44).

In Figure 8 we compare *in-situ* SANS profiles of P4(44), P9(53), and P17(42) obtained at RH = 95% and 60 °C. We see the $1q^*$, $\sqrt{3}q^*$, $\sqrt{4}q^*$, $\sqrt{7}q^*$, $\sqrt{9}q^*$, $\sqrt{11}q^*$, and $\sqrt{12}q^*$ Bragg reflections with $q^* = 0.14$ nm^{-1} for P17(42) as shown by inverted arrows (⇓), the $1q^*$, $\sqrt{3}q^*$, $\sqrt{4}q^*$, $\sqrt{7}q^*$, $\sqrt{9}q^*$, $\sqrt{11}q^*$, $\sqrt{12}q^*$, $\sqrt{16}q^*$, and $\sqrt{24}q^*$ Bragg reflections with $q^* = 0.28$ nm^{-1} for P9(53) as shown by inverted open triangles (▽) arrows, and the $1q^*$, $\sqrt{3}q^*$, and $\sqrt{4}q^*$ Bragg reflections with $q^* = 0.54$ nm^{-1} for P4(44) as shown by inverted filled triangles (▼). The SANS data indicate the presence of HEX phase with domain spacing 44.9, 22.4, and 11.6 nm for hydrated P17(42), P9(53), and P4(44),

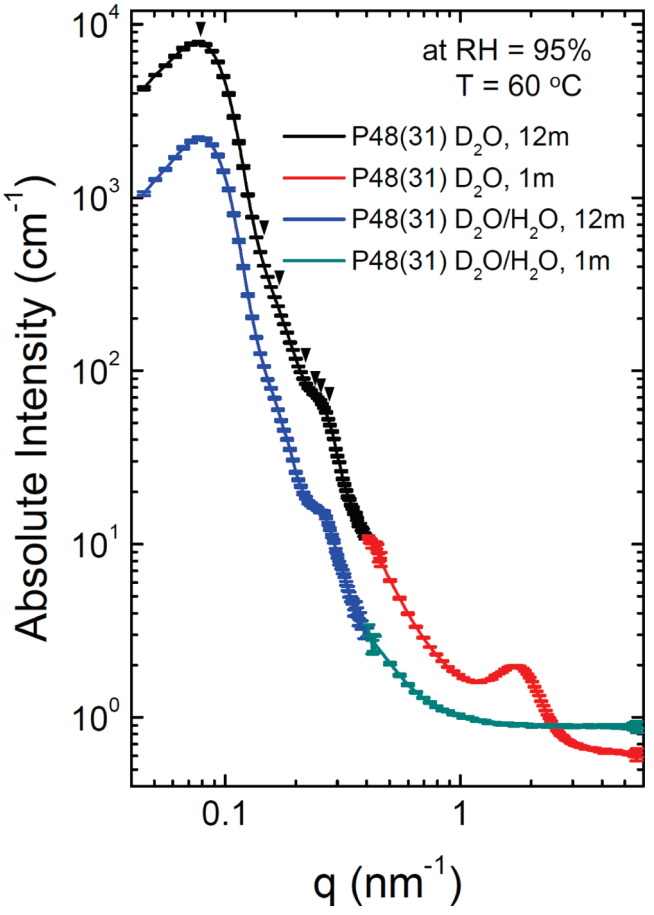

Figure 6. *In-situ* SANS intensity versus magnitude of the scattering vector, q, of P48(31) obtained at RH = 95% and 60 °C with (a) 100% D_2O and (b) 32/68 volumetric D_2O/H_2O mixture. Bragg peaks at $1q^*$, $\sqrt{3}q^*$, $\sqrt{4}q^*$, $\sqrt{7}q^*$, $\sqrt{9}q^*$, $\sqrt{11}q^*$, and $\sqrt{12}q^*$ are indicated by the inverted filled triangles (▼).

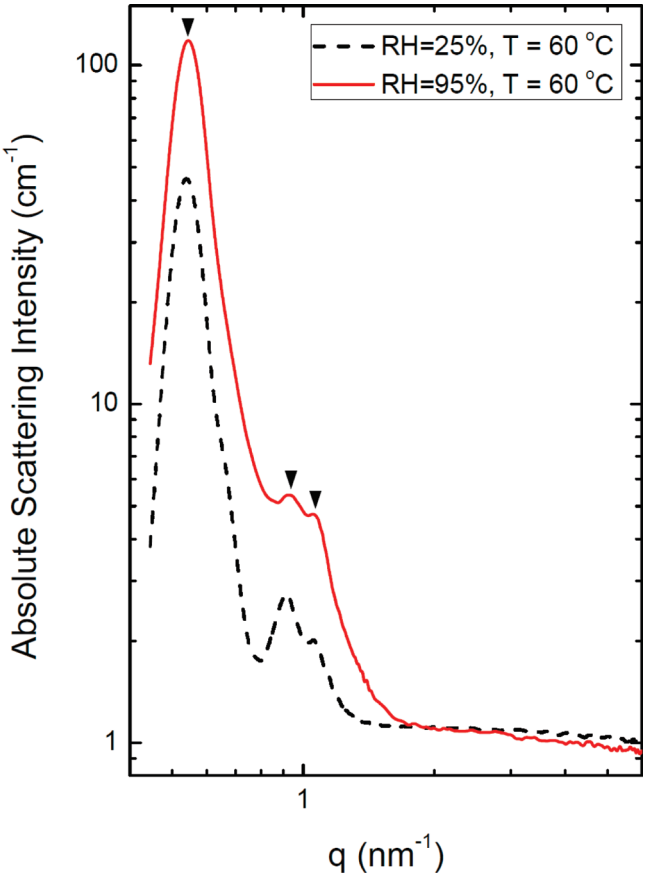

Figure 7. *In-situ* SANS intensity versus magnitude of the scattering vector, q, of hydrated P4(44) obtained at RH = 95% and 60 °C (solid curve) and dry P4(44) at RH = 25% and 60 °C (dashed curve). Both profiles show Bragg peaks (▼) at $1q^*$, $\sqrt{3}q^*$, and $\sqrt{4}q^*$, indicative of the HEX phase. The lack of a water peak in the vicinity of $q = 1.8$ nm^{-1} in the hydrated state implies the presence of homogeneous hydrophilic PSS domains.

respectively. The coexistence of microphase (larger length scale) and water domain (smaller length scale) is seen for the P17(42) and P9(53) as highlighted with blue shadow in Figure 8. It is worthwhile to note that the spacing between water domains is not a sensitive function of the width of hydrophilic PSS domains. For example, although the PSS domain width of P17(42) (22 nm) is twice as large as that of P9(53) (11 nm), two samples reveal very similar water channel spacing as 3.0 and 3.1 nm, respectively. It is evident that there exists a critical size of the nominally hydrophilic domain below which the water domains are homogenized. For PSS−PMB copolymers with SL = 47 ± 6%, this cutoff lies between 6 and 10 nm.

In Figure 9, we plot d_{water} versus SL for all of the PSS-*b*-PMB samples that exhibited a water peak. It is evident that d_{water} depends mainly on SL and not on the size or spacing of the nominally hydrophilic PSS domains until they are thinner than the 6 nm cutoff. There are many possible explanations for the existence of a cutoff below which the water domains are absent. The heterogeneity of the hydrated domains undoubtedly arises due to the close proximity of hydrophilic and hydrophobic moieties. In fact, one might even consider that polystyrene portion of the hydrophilic monomers to be hydrophobic. The formation of watery domains reduces the unfavorable contacts between water and the hydrophobic portions of the PSS chains but introduces concentration gradients between the water-rich and water-poor domains. Theoretical frameworks proposed by van der Waals[32] and Cahn and Hilliard[33] can be used to evaluate the free energy penalty due to the presence of concentration gradients. Confining mixtures to small regions results in the reduction of the gradients because of the increasing importance of the gradient free energy penalty, relative to the free energy gain of separating the components. In the case of binary mixtures that are phase separated in the bulk, confinement results in homogenization if the length scale of the confinement is below a well-defined cutoff.[34] We propose that similar effects are responsible for the observed cutoff for randomly sulfonated block copolymers when the hydrophilic PSS domain width approaches 6 nm. The 3−5 nm water domain spacing observed more or less universally in PEMs probably represents a balance between enthalpic gains due to a decrease in contacts between hydrophobic portions of the chains and water and the gradient free energy penalty associated with the formation of watery domains in the absence of finite size effects. It is evident that the homogeneous hydrophilic PSS phases with characteristic widths less than 6 nm are more effective for retaining water at elevated temperatures and for promoting proton transport.

We conclude this section commenting on the ramifications of our work on the structure of widely studied randomly sulfonated homopolymers such as Nafion and SPEEK. Whether the formations of watery domains in randomly sulfonated homopolymers and randomly sulfonated block copolymers are similar in origin or not remains an interesting open question.[35] There are, however, two important similarities in the scattering data obtained from these two systems that suggest that the origin is similar:

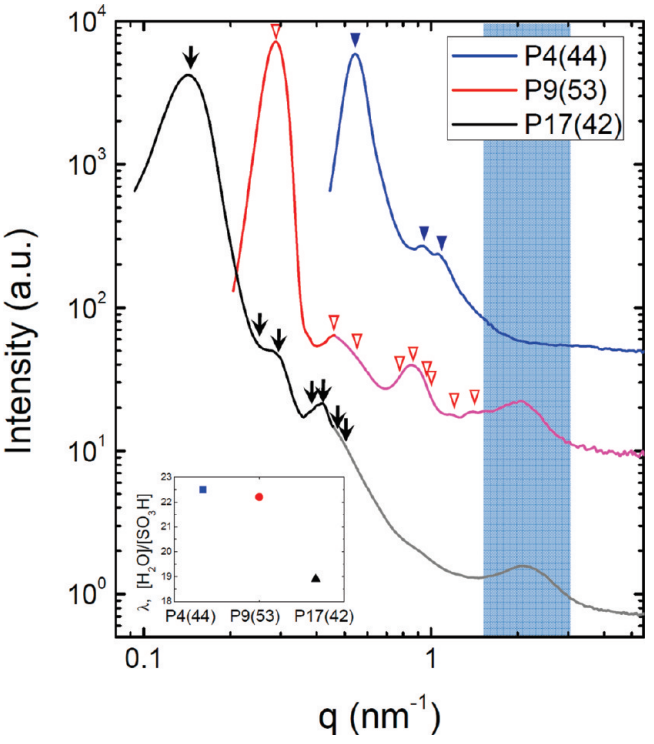

Figure 8. *In-situ* SANS intensity versus magnitude of the scattering vector, q, of P4(44), P9(53), and P17(42) obtained at RH = 95% and 60 °C. The inverted filled triangles (▼) of P4(44), the inverted open triangles (▽) of P9(53), and the arrows (↓) of P17(42) indicate Bragg peaks with ratio of 1, √3, and √4; of 1, √3, √4, √7, √9, √11, √12, √16, and √24; and of 1, √3, √4, √7, √9, √11, and √12, respectively. The scattering profiles of P9(53) and P4(44) are offset vertically by factors of 10 and 50, respectively. Inset plot shows degree of hydration, λ, of samples.

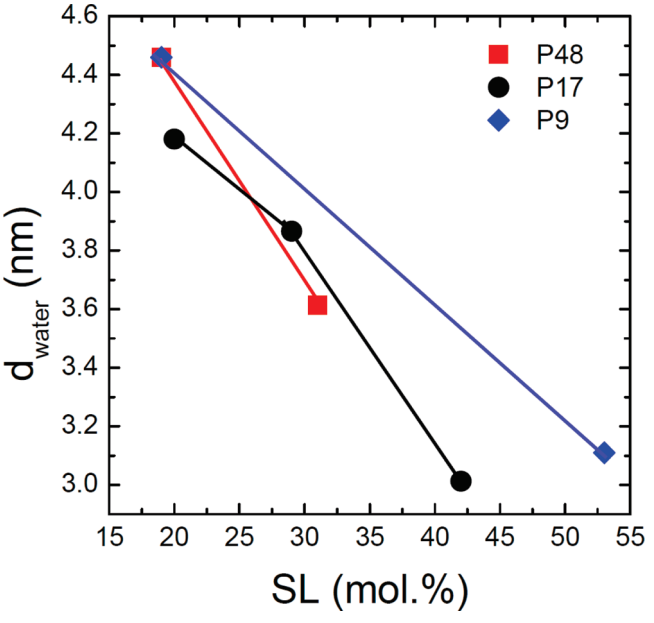

Figure 9. Water domain spacing d_{water} vs SL for different randomly sulfonated PSS-*b*-PMB block copolymers.

(1) The fact that the water peak is seen in the same location (d_{water} between 3 and 5 nm) in both randomly sulfonated homopolymers and block copolymers. (2) If one disregards the modulations from the Bragg reflections, the rapid decay in low-angle scattering are similar in both randomly sulfonated homopolymers and block copolymers. In the case of the block copolymers it is clear that the d_{water} is unrelated to the spacing between the hydrophilic PSS domains. In fact, in the case of the most conductive block copolymer, P4(44), the water peak was absent. The most logical conclusion is thus that the arrangement of the watery domains in randomly sulfonated homopolymers is entirely aperiodic with no well-defined length scale. The only length scale in these materials arises from the formation of a water-rich and water-poor substructure within the nominally hydrophilic domains as proposed by Nieh et al.[19]

Conclusion

We have studied hydrated morphology of PSS-*b*-PMB block copolymer electrolyte membranes in equilibrium with humidified air using *in-situ* SANS. Our experiments cover a wide range of sulfonation levels, copolymer molecular weight, temperature, and relative humidity. The existence of several higher order peaks in the SANS data enables quantitative determination of the arrangement of the nominally hydrophilic PSS domains that form the matrix of microphases. We demonstrate that the nominally hydrophilic PSS domains contain a substructure periodically arranged water-rich domains with a characteristic length scale d_{water}. This length scale is unrelated to the spacing between the hydrophilic PSS domains as long as that spacing exceeds 10 nm and decreases with increasing sulfonation level of the PSS chains. The watery domain substructure ceases to exist when the spacing between the hydrophilic PSS domains is decreased to 6 nm over the entire range of temperature and relative humidity investigated. Homogeneous water distribution within the nominally hydrophilic PSS domains may be responsible for the rapid proton transport seen in low molecular weight PSS−PMB copolymers.[29]

Acknowledgment. This research was supported by Basic Science Research Program through the National Research Foundation of Korea (NRF) funded by the Ministry of Education, Science and Technology (Project No. 2010-0007798) and WCU (World Class University) program through the Korea Science and Engineering Foundation funded by the Ministry of Education, Science and Technology (Project No. R31-2009-000-10059-0). The SANS facilities at NIST are supported in part by the National Science Foundation under Agreement DMR-0504122.

References and Notes

(1) Hickner, M. A.; Ghassemi, H.; Kim, Y. S.; Einsla, B. R.; McGrath, J. E. *Chem. Rev.* **2004**, *104*, 4587.
(2) Mauritz, K. A.; Moore, R. B. *Chem. Rev.* **2004**, *104*, 4535.
(3) Kreuer, K. D. In *Handbook of Fuel Cell − Fundamentals, Technology and Applications*; Vielstich, W., Lamm, A., Gasteiger, H. A., Eds.; John Wiley & Sons Ltd.: Chichester, UK, 2003; Vol. *3*, Part 3.
(4) Wu, D.; Paddison, S. J.; Elliott, J. A. *Macromolecules* **2009**, *42*, 3358.
(5) Kopitzke, R. W.; Linkous, C. A.; Anderson, H. R.; Nelson, G. L. *J. Electrochem. Soc.* **2000**, *147*, 1677–1681.
(6) Yoonessi, M.; Dang, T. D.; Heinz, H.; Wheeler, R.; Bai, Z. *Polymer* **2010**, *51*, 1585.
(7) Register, R. A.; Sen, A.; Weiss, R. A.; Cooper, S. L. *Macromolecules* **1989**, *22*, 2224.
(8) Register, R. A.; Cooper, S. L. *Macromolecules* **1990**, *23*, 318.
(9) Gebel, G.; Moore, R. B. M. *Macromolecules* **2000**, *33*, 4850–4855.
(10) Kreuer, K. D.; Schuster, M.; Obliers, B.; Diat, O.; Traub, U.; Fuchs, A.; Klock, U.; Paddison, S. J.; Maier, J. *J. Power Sources* **2008**, *178*, 499–509.
(11) Gebel, G.; Lambard, J. *Macromolecules* **1997**, *30*, 7914–7920.
(12) Rubatat, L.; Rollet, A. L.; Gebel, G.; Diat, O. *Macromolecules* **2002**, *35*, 4050–4055.
(13) Kreuer, K. D. *J. Membr. Sci.* **2001**, *185*, 29–39.
(14) Schmidt-Rohr, K.; Chen, Q. *Nature Mater.* **2008**, *7*, 75–83.
(15) Gierke, T. D.; Munn, G. E.; Wilson, F. C. *J. Polym Sci., Part B: Polym. Phys.* **1981**, *19*, 1687–1704.

(16) Haubold, H. G.; Vad, Th.; Jungbluth, H.; Hiller, P. *Electrochim. Acta* **2001**, *46*, 1559–1563.
(17) Krivandin, A. V.; Solov'eva, A. B.; Glagolev, N. N.; Shatalova, O. V.; Kotova, S. L. *Polymer* **2003**, *44*, 5789–5796.
(18) Kim, M.-H.; Glinka, J. C.; Grot, S. A.; Grot, W. G. *Macromolecules* **2006**, *39*, 4775–4787.
(19) Nieh, M. P.; Guiver, M. D.; Kim, D. S.; Ding, J. F.; Norsten, T. *Macromolecules* **2008**, *41*, 6176–6182.
(20) Elabd, Y. A.; Napadensky, E.; Walker, C. W.; Winey, K. I. *Macromolecules* **2006**, *39*, 399–407.
(21) Kim, J.; Kim, B.; Jung, B. *J. Membr. Sci.* **2002**, *207*, 129–137.
(22) Shi, Z.; Holdcroft, S. *Macromolecules* **2005**, *38*, 4193–4201.
(23) Rubatat, L.; Shi, Z.; Diat, O.; Holdcroft, S.; Frisken, B. J. *Macromolecules* **2006**, *39*, 720–730.
(24) Weiss, R. A.; Sen., A.; Pottick, L. A.; Willis, C. L. *Polymer* **1991**, *32* (15), 2785–2792.
(25) Mani, S.; Weiss, R. A.; Williams, C. E.; Hahn, S. F. *Macromolecules* **1999**, *32*, 3663–3670.
(26) Zhou, N. C.; Xu, C.; Burghardt, W. R.; Composto, R. J.; Winey, K. I. *Macromolecules* **2006**, *39*, 2373.
(27) Park, M. J.; Balsara, N. P. *Macromolecules* **2008**, *41*, 3678–3687.
(28) Leibler, L. *Macromolecules* **1980**, *13*, 1602.
(29) Park, M. J.; Downing, K. H.; Jackson, A.; Gomez, E. D.; Minor, A. M.; Cookson, D.; Weber, A. Z.; Balsara, N. P. *Nano Lett.* **2007**, *7*, 3547.
(30) Wang, X.; Yakovlev, S.; Beers, K. M.; Park, M. J.; Mullin, S. A.; Downing, K. H.; Balsara, N. P. *Macromolecules* **2010**, *43*, 5306–5314.
(31) Lefelar, J. A.; Weiss, R. A. *Macromolecules* **1984**, *17*, 1145–1158.
(32) Rowlinson, J. S. *J. Stat. Phys.* **1979**, *20*, 197–200.
(33) Cahn, J. W.; Hilliard, J. E. *J. Chem. Phys.* **1958**, *28*, 258–266.
(34) Akpalu, Y. A.; Karim, A.; Satija, S. K.; Balsara, N. P. *Macromolecules* **2001**, *34*, 1720–1729.
(35) Roche, E. J.; Pineri, M.; Duplessix, R.; Levelut, A. M. *J. Polym. Sci., Polym. Phys. Ed.* **1981**, *19*, 1–11.
(36) Certain commercial equipment, instruments, or materials (or suppliers, or software) are identified in this paper to foster understanding. Such identification does not imply recommendation or endorsement by the National Institute of Standards and Technology, nor does it imply that the materials or equipment identified are necessarily the best available for the purpose.